X-693-75-99
PREPRINT

THE SOLAR ELONGATION DISTRIBUTION OF LOW FREQUENCY RADIO BURSTS

M. L. KAISER

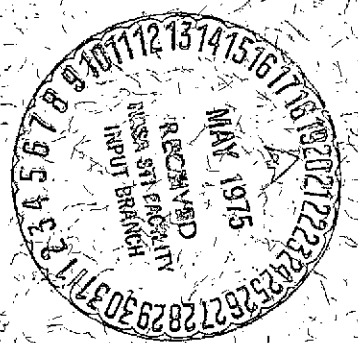

APRIL 1975

GSFC
GODDARD SPACE FLIGHT CENTER
GREENBELT, MARYLAND

For information concerning availability
of this document contact:

Technical Information Division, Code 250
Goddard Space Flight Center
Greenbelt, Maryland 20771

(Telephone 301-982-4488)

THE SOLAR ELONGATION DISTRIBUTION OF LOW FREQUENCY RADIO BURSTS

by

M.L. Kaiser
Radio Astronomy Branch
Laboratory for Extraterrestrial Physics
Goddard Space Flight Center
Greenbelt, Maryland USA

ABSTRACT

Over 500 days of low frequency (<5 MHz) radio observations from the IMP-6 spacecraft have been accumulated to produce a two dimensional map (frequency versus elongation) of solar type III burst occurrences. This map indicates that most solar bursts are emitted at the second harmonic of the plasma frequency rather than the fundamental. The map also shows that the solar wind electron density varies as $R^{-\gamma}$ where $2 \leq \gamma \leq 3$.

The question of whether solar fast-drift radio bursts (type III) emit their radiation at the fundamental or the second harmonic (= $2f_o$) of the solar wind plasma frequency is important in assessing the viability of the several current theories on type III mechanisms. For the past several years, spacecraft observations of these bursts at low frequency (<5 MHz) have given indirect evidence that emission occurs at the second harmonic (see Fainberg and Stone, 1974). In this paper, data from the Goddard Space Flight Center's radio astronomy experiment on board the IMP-6 spacecraft have been analyzed to search for a predicted geometrical effect which could provide additional evidence on this problem.

If the angular distances from the Sun of type III solar bursts at a given frequency are collected over a long period of time, there will be an elongation angle beyond which bursts are rarely seen. This maximum angle corresponds to a viewing direction tangent to the relevant plasma level; the solar limb for that frequency. A simplified version of this geometry is shown in Figure 1a. The plane of the figure is the ecliptic and a plasma level corresponding to a particular plasma frequency is shown as a heliocentric circle of radius P. A burst occurring at this plasma level and a central meridian longitude angle θ will be measured at Earth as occurring at elongation ϕ. When

the sum of ϕ and θ are 90^{o}, the elongation ϕ reaches maximum and additional increases in θ are either observed at lower elongation angles, or, more likely, not observed at all due to propagation difficulties.

If the observed occurrence rate of bursts as a function of elongation were measured, there would not only be a maximum elongation, but also an enhancement in the distribution near this maximum. This enhancement is due to foreshortening and can be seen numerically in Figure 1b. Here, the rate of change of longitude as a function of elongation is plotted against elongation for several plasma levels. For example, at a plasma level of 0.5 AU (corresponding to a very low plasma frequency) the maximum elongation is 30^{o}, which occurs at a longitude of 60^{o}. However, when the elongation angle is 25^{o}, bursts are produced at a longitude of $32^{o}.7$, so that the outermost 5^{o} of the distribution integrates over $27^{o}.3$ in longitude. If we assume bursts are produced uniformly in longitude this effect will cause a large enhancement in the distribution at the limb.

In principle, observations of these limb enhancements as a function of observing frequency could be used to decide if solar bursts are generated at the fundamental or the second harmonic of the plasma frequency, and possibly to determine the average solar wind electron density as a function of radial distance. However,

there are a number of complications which must be considered before conclusions can be drawn from actual observations.

The first problem is the expansion of the simple geometry of Figure 1 to three dimensions, where the plasma levels become spheres. A burst occurring on a particular sphere has both a longitude and latitude component, each of which will also have maximum values analogous to the two-dimensional case. The total number of bursts at a given elongation is then a double integral over some range of solar latitude and longitude. The general effect will be to enhance the center of the elongation distribution relative to the limbs. This will be particularly important close to the Sun because the maximum latitude dictated by the line-of-sight tangent to the plasma level sphere is large.

A second consideration is the effect of varying distance from the point of emission to the observer. The observed flux varies inversely with the square of distance, but the variation of the number distribution is more subtle. The observations discussed in this paper and similar observations discussed by Fitzenreiter et al. (1975) show that solar bursts are distributed in a form

$$n(F) \propto F^{-\beta}$$

where n is the number of bursts of a given flux, F, and β varies between 1.25 a very low frequencies ($\sim$100 kHz) to perhaps 1.75 at

5 MHz. If each point on the plasma sphere shows a similar flux distribution, then the contribution to the elongation distribution is

$$N_o \propto \int_t^\infty F^{-\beta}\, dF,$$

where t is the detection threshold. At a distance R this contribution would be changed by

$$\frac{N_R}{N_o} = \left(\frac{R_o}{R}\right)^{2(\beta-1)}$$

At a plasma level of 0.5 AU, the ratio N_R/N_o is never less than 0.80, thus at higher frequencies, with plasma levels closer to the Sun, the distance effect is negligible. However, at lower frequencies, the distance differential becomes more important. This effect also tends to reduce the limb-to-center ratio in the elongation distribution.

A general smearing or broadening of the distribution will result from variations in the solar wind electron density. Montgomery et al. (1972) indicates that in situ observations show a scatter of 50% around the mean electron density at 1 AU. This is equivalent to approximately 20% variation in the position of plasma levels.

An attempt to depict the elongation distribution resulting from these considerations is shown in Figure 2. The left panel (2a) shows the predicted elongation distribution for three plasma levels, taking into account a three-dimensional plasma sphere, an R^{-1} and $R^{-1/2}$ ($\beta = 1.5$ and 1.25) source-to-observer distance correction, and a

$\pm$ 20% plasma level variation (one sigma level of a normal distribution). The expected limb-to-center de-emphasis, caused mostly by the inclusion of three dimensions, can be easily seen at the $36R_\odot$ level and the broadening is evident at all levels. The differential distance correction is noticeable only at $191R_\odot$.

Several assumptions are implicit in Figure 2, the most important of which is the presumption that solar bursts occur at a uniform rate at all points on the plasma level sphere. Inclusion of arbitrary cutoffs in solar latitude produce central holes in the distribution, particularly at plasma levels close to the Sun. However, at lower frequencies (plasma levels ≥ 0.75 AU) where the emphasis of this study lies, the latitude at the line-of-sight tangent is less than 40°, so no latitude cutoff was used in the numerical simulation. Also, no attempt was made to include the effects of scattering or any intrinsic beaming of emission.

Figure 2b shows the numerical prediction of solar burst distribution for plasma levels from the Sun to very near the Earth. The distribution peak at each plasma level is normalized to 100%, and the contours are drawn relative to the peaks. A very broad limb enhancement can be seen from $200R_\odot$ until it merges into a central peak at around $30R_\odot$. The point of this study is to try to observe this limb enhancement and to relate the plasma levels to observing frequency.

The Goddard Space Flight Center radio astronomy experiment onboard the IMP-6 spacecraft was used in an effort to make these observations. The experiment, described in detail by Brown (1973), consisted of two 32-channel radiometers connected to a 90-m dipole and operated between 30 kHz and 9.9 MHz. The IMP-6 was spin stabilized, with the dipole antenna lying in the spin plane, which was parallel to the ecliptic plane. Even at these very long wavelengths, the direction of emission was accurately measured by cross-correlation between the dipole antenna pattern and the imposed spin modulation pattern. This has proved to be a powerful technique for low-frequency solar work as shown by Fainberg et al. (1973).

The data processing approach used to study the limb enhancements was to stack all data from IMP-6 in Sun-centered elongation coordinates. It was reasoned that over a long period of time non-solar events would scatter when stacked in this way and the repeatable solar scans would be enhanced. A major exception to this philosophy was an extensive effort to eliminate obvious terrestrial emissions (see Kaiser and Stone, 1975) by excluding all data taken when the spacecraft was inside the Earth's magnetosphere as well as any emission originating within 7.5 Earth radii of the Earth. This Earth filtering eliminated typically 90% of the IMP-6 data. However, even with this extreme reduction about 10^6 five-second data samples spread over 500 days (May 1971-Oct 1972)

remained for use in this study.

Specifically, the data were accumulated in two-degree solar-elongation bins determined by the emission direction (as deduced from spin-modulation measurements over three-minute processing windows). This resulted in a histogram for each observing frequency of some arbitrary "number of events" versus elongation. As a check on the validity of this overall data processing method, these histograms were compared to histograms of selected solar type III events culled from the same IMP-6 data base by Fitzenreiter et al. (1975). The two methods appeared to produce nearly identical histograms, thereby justifying the data-processing method used in this paper.

Figure 3 is the result of this 500-day accumulation displayed in a manner similar to Figure 2b with contours again relative to the peaks. Both eastern and western elongations are shown, whereas, in Figure 2b, symmetry is implied.

Note that Figures 2b and 3 can be aligned only if we set 1 AU ($\equiv 215 R_\odot$) approximately equal to 50 kHz. In situ solar wind measurements at 1 AU (Montgomery, et al. 1972) indicate a plasma frequency of approximately 25 kHz; thus, Figure 3 strongly suggests that most low-frequency solar emission occurs at the second harmonic of the plasma frequency as suggested by earlier measurements (see Fainberg and Stone, 1974).

The shaded curves marked A and B illustrate this point even better. Curve A was made by assuming that emission occurs at the plasma frequency, which is fixed at 25 kHz near the Earth. Curve B results if emission occurs at the second harmonic. The boundaries of curves A and B are formed by solar-wind density functions proportional to R^{-2} (inner edge) and $R^{-2.63}$ (outer edge). The second harmonic interpretation is strongly favored over curve A particularly at western elongations.

The other goal of this research was to determine the solar wind electron density as a function of distance. Fainberg and Stone (1971) have determined an electron density scale proportional to $R^{-2.63}$ for a particular radio storm in August 1968. The lower boundaries of the shaded areas represent this type of function and it does appear for curve B to follow the contours. However, the upper boundary of B, which is an $N_e \propto R^{-2}$ function, also follows the contours. It therefore appears, not too surprisingly, that averaged over 500 days, the electron density scale varies considerably. There is evidence that this data processing method can be used to determine electron density scales for particular active regions and this type of investigation will be pursued.

Figure 3 indicates a small but systematic asymmetry between the eastern and western halves of the distribution. The "limb" in

the east seems to be at a slightly smaller elongation (relative to 0°) than the west. Also, at higher frequencies, the center of the distribution is marginally displaced toward the west.

The cause of the western excess is not known. It is possible that, over the sample time period, more bursts were produced in the west than the east. However, 500 days seems rather long for an effect of this type to persist. In fact, the only known solar feature which shows an east-west asymmetry over long time periods is the magnetic field. Our line of sight intersects the Archimedean spiral differently in the west than in the east. Thus, any type of emission beaming (intrinsic or imposed by propagation) related to the magnetic field could cause the distribution shown in figure 3.

The low-frequency central peak that is observed, but was not predicted, can be numerically accounted for with more smearing. Two likely candidates for this smearing are the finite receiver bandwidth (10 kHz) which becomes, at low frequencies, a sizeable fraction of the observing frequency, and scattering, which becomes more important as observing frequencies approach the local plasma frequency.

In summary, a rather simple data-processing technique has been employed to study the distribution in elongation of type III solar bursts. This study indicates that, at low frequencies, most bursts occur at the

second harmonic of the plasma frequency, rather than at the fundamental. Also, the solar wind electron density scale appears to be within boundaries of $1/R^2$ to $1/R^3$.

REFERENCES

Brown, L.W.: 1973, Astrophys. J. 180, 359.

Fainberg, J., and Stone, R.G.: 1971, Solar Physics 17, 392.

Fainberg, J., Evans, L.G., and Stone, R.G.: 1972, Science 178, 743.

Fainberg, J., and Stone, R.G.: 1974, Spa. Sci. Rev. 16, 145.

Fitzenreiter, R.J., Fainberg, J., and Malitson, H.H.: 1975, in preparation.

Kaiser, M.L., and Stone, R.G.: 1975, Science, in press.

Montgomery, M.D , Bame, S.J., and Hundhausen, A.J.: 1972, J. of Geophys. Res., 77, 5432.

Figure Captions

Fig. 1a. A type III burst occurring at a distance P from the Sun will have an elongation angle ϕ as seen from the Earth and longitude θ as seen from the Sun.

Fig. 1b. The rate of change of longitude as a function of elongation for various distances from the Sun.

Fig. 2a. The predicted distribution of solar bursts at three levels taking into account three dimensions, varying source-observer distance and local electron density fluctuations.

Fig. 2b. Contours of equal distribution relative to the peak at each plasma level between the Earth and Sun.

Fig. 3. The result of accumulation of 500 days of IMP-6 data in solar elongation coordinates. Contours are analogous to those of figure 2b.

TWO - DIMENSIONAL SOLAR LIMB ENHANCEMENT

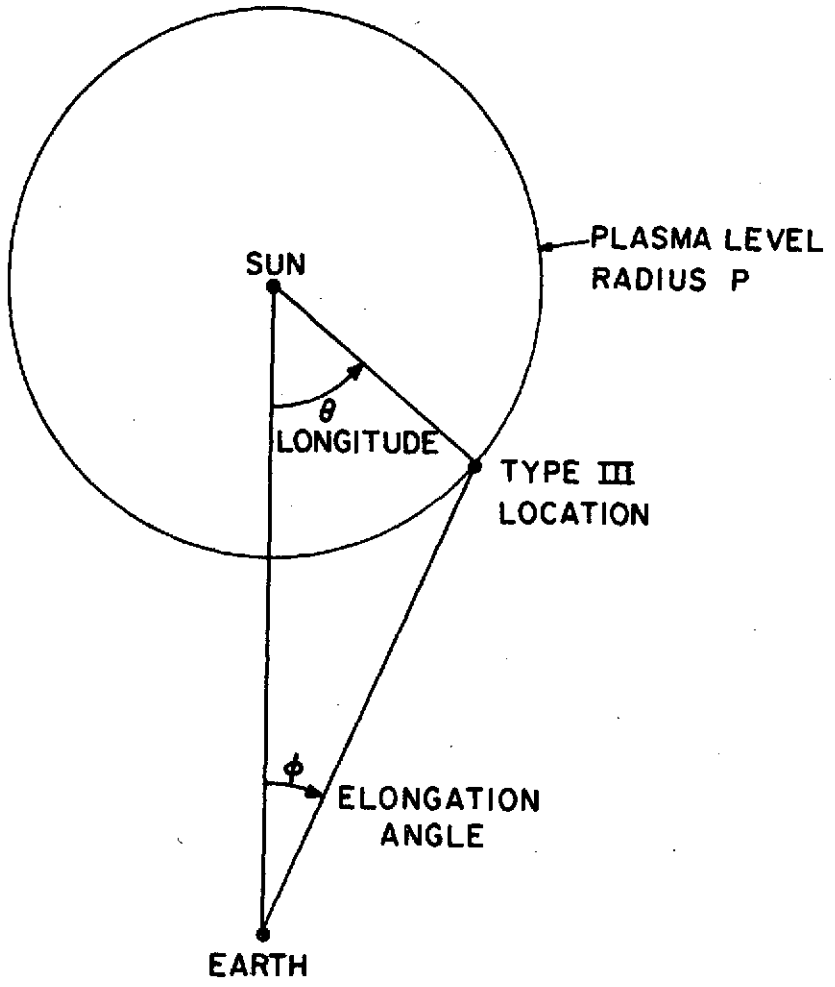

(a)

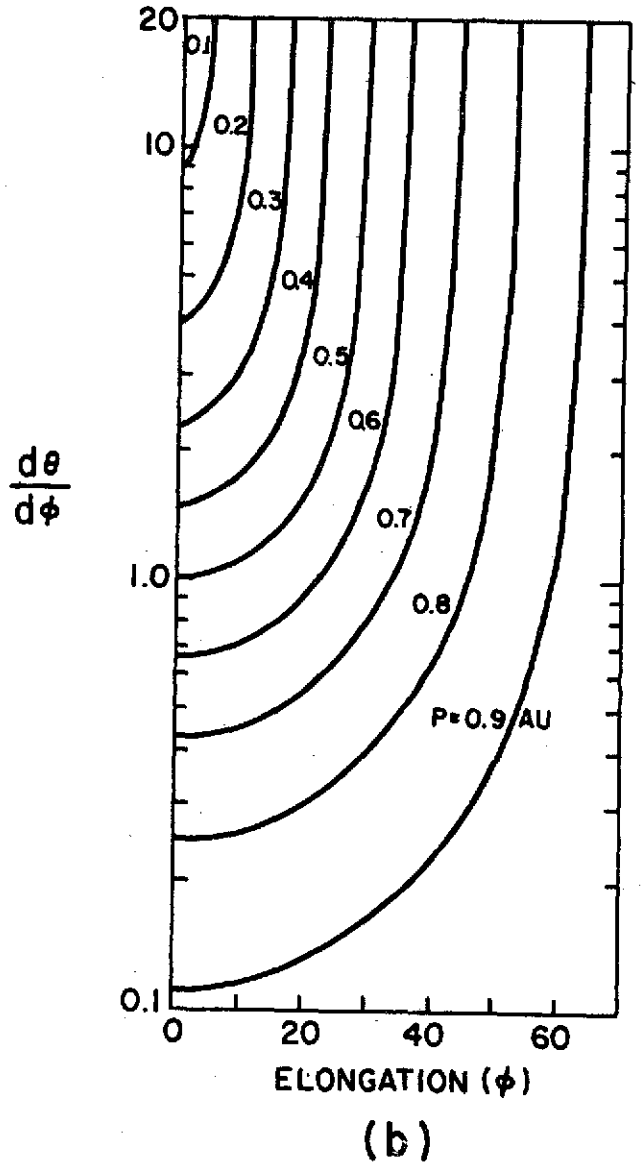

(b)

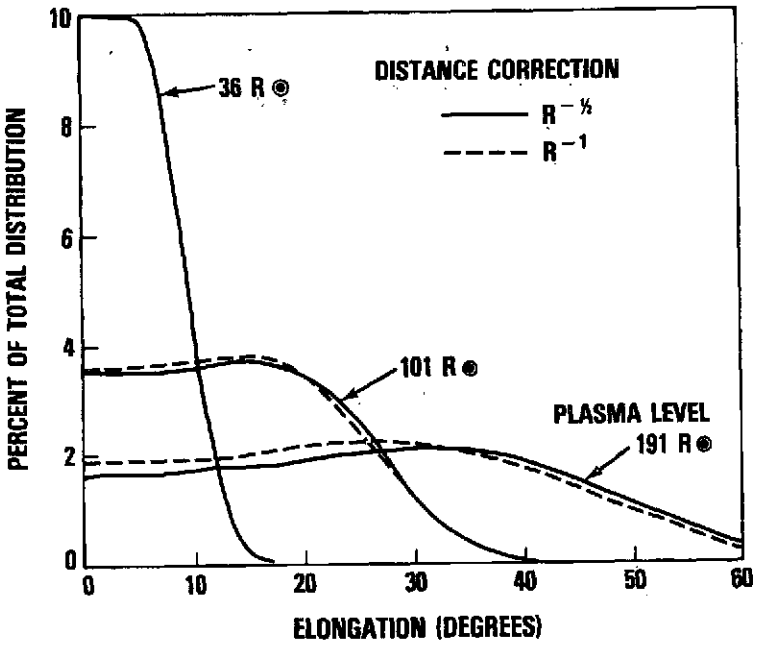
PERCENT OF TOTAL DISTRIBUTION
10
8
6
4
2
0
0
10
20
30
40
50
60
ELONGATION (DEGREES)
36 R⊙
DISTANCE CORRECTION
R^-½
R^-1
101 R⊙
PLASMA LEVEL
191 R⊙

(a)

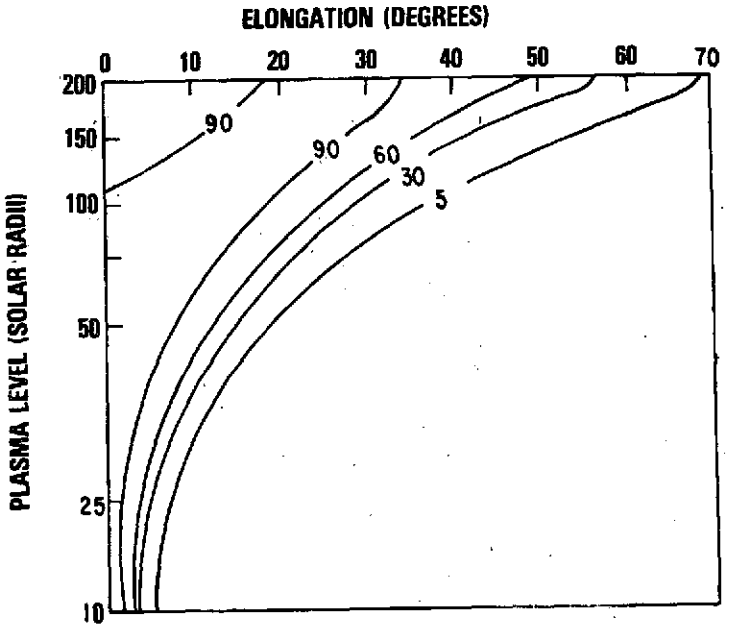
ELONGATION (DEGREES)
0
10
20
30
40
50
60
70
PLASMA LEVEL (SOLAR RADII)
200
150
100
50
25
10
90
90
60
30
5

(b)

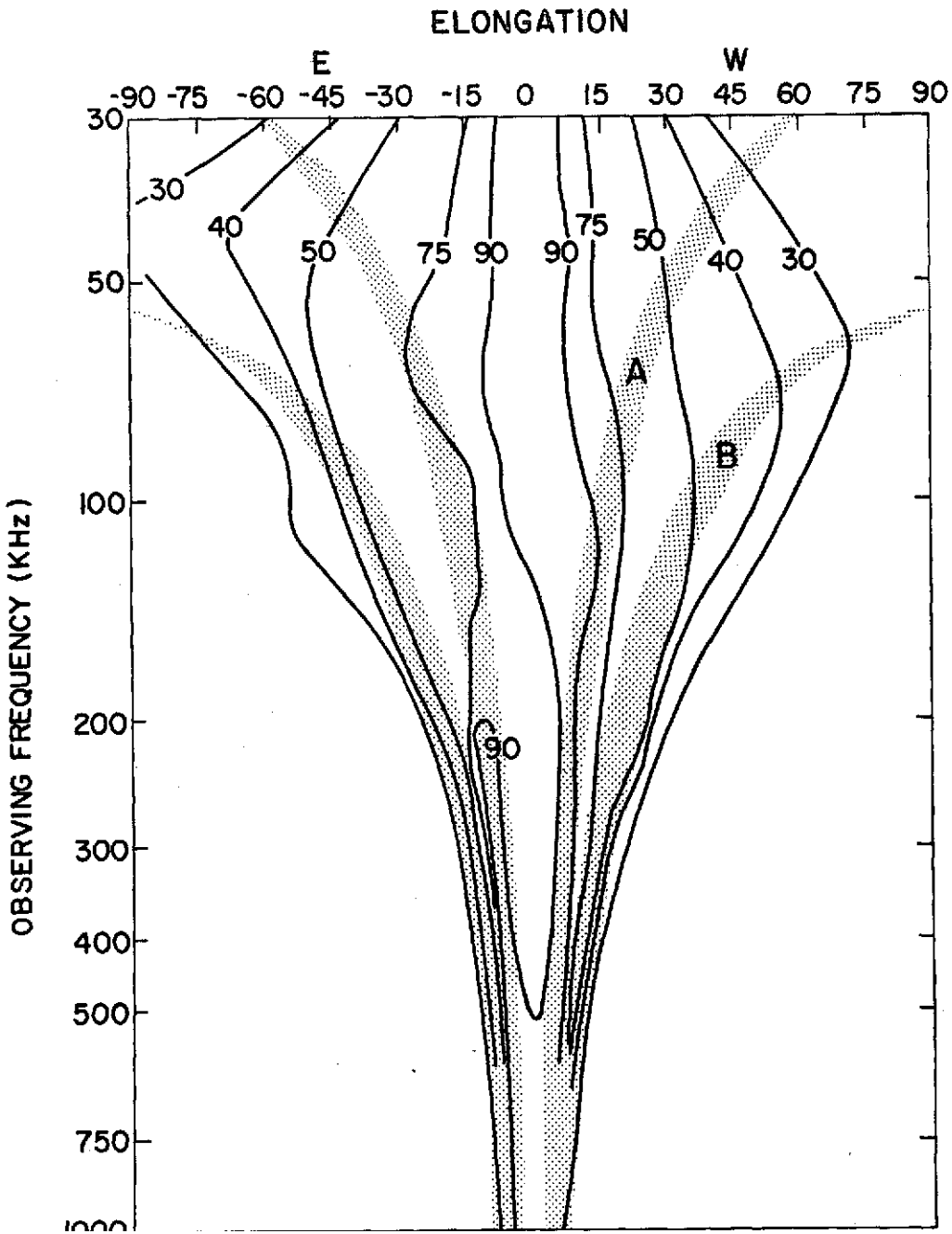
ELONGATION
E
W
-90 -75 -60 -45 -30 -15 0 15 30 45 60 75 90
30
50
100
200
300
400
500
750
OBSERVING FREQUENCY (KHz)
30
40
50
75
90
90
75
50
40
30
90
A
B